

IEN-CsF1 TAI EVALUATION

MJD 53639-53664 (September the 26th–October the 21st 2005)

Introduction

During the period MJD 53639.0-53664.0, IEN has evaluated the frequency of its Hydrogen Maser IEN-HM2 (BIPM code 1401102) using the Cs fountain primary frequency standard IEN-CsF1. The evaluation procedure of the fountain standard follows the general procedures reported in [1]; we report here details on the Type A and Type B uncertainty evaluation, together with the internal transfer uncertainty (including the contribution of dead time).

The experimental set-up is not changed with respect to the last measurement (period MJD 53584.0-53624.0). The measurement procedure is unchanged but the evaluation of the collisional shift.

IEN-CsF1 Accuracy Evaluation

Black Body Radiation Shift $\Delta\nu_{\text{BBR}}$

The evaluation of the Blackbody Radiation (BBR) Shift $\Delta\nu_{\text{BBR}}$ requires to know the effective BBR temperature T experienced by the atoms along their ballistic flight. For the calculation of T , we interpolate the temperature data coming from four thermocouples positioned along the drift tube with a polygonal curve and then we calculate the average radiation temperature experimented by the atoms at a given position (integrated over the solid angle); in this way it is possible to take into account also the effect of the two “holes” in the blackbody radiator, the upper window and the hole in the microwave cavity. The values obtained at different elevations inside the fountain drift tube are then used to calculate the time averaged radiation temperature seen by the atoms along their ballistic flight. See the discussion reported in [2] for details.

To evaluate $\Delta\nu_{\text{BBR}}$ from the effective temperature T we follow the well known relation discussed for example in [2] and reported here below; the leading coefficient β here used is calculated using results presented in [3]; the coefficient ε is taken from [4].

$$\Delta\nu_{\text{BBR}} = \beta (T/300)^4 \cdot [1 + \varepsilon(T/300)^2]$$

$$\beta = (-1.711 \pm 0.003) \cdot 10^{-14}$$

$$\varepsilon = 0.014$$

$$T = 70.3 \pm 0.3 \text{ }^\circ\text{C} = 343.4 \pm 0.3 \text{ K}$$

$$\Delta\nu_{\text{BBR}} = (-29.9 \pm 0.1) \cdot 10^{-15}$$

Gravitational Red Shift $\Delta\nu_{\text{RS}}$

The absolute orthometric height (h) of the IEN-CsF1 location is calculated using a geodetic height and a Geoid model. The geodetic height with respect to the ellipsoid WGS84 is provided by the IEN GPS geodetic receiver. The Geoid height (EGM96) with respect to the WGS84 coordinate

was calculated using the National Geospatial-Intelligence Agency (NGA) EGM96 Geoid calculator, available at the URL <http://earth-info.nga.mil/GandG/wgs84/gravitymod/egm96/intpt.htm>. The height difference between the GPS antenna position and the fountain location was obtained as a result of a direct measurement. Reference for the proportional coefficient γ value is [5].

$$\Delta v_{RS} = \gamma \cdot h$$

$$\gamma = 1.09 \cdot 10^{-16} \text{ m}^{-1}$$

$$h = 242 \pm 1 \text{ m}$$

$$\Delta v_{RS} = (26.4 \pm 0.1) \cdot 10^{-15}$$

Quadratic Zeeman Shift Δv_z

The effective C-field experienced by the atoms (B_0) along their trajectory is calculated (see [1] for details) from a field map which is obtained measuring the low frequency magnetic resonance transitions when the atoms are at the apogee; the map is completed launching the atoms at different apogee heights.

The C-field map obtained immediately after this evaluation period is reported in the figure 1 and it was used to calculate the quadratic Zeeman shift by mean of a field integration over the flight time. Reference for the value of the quadratic Zeeman constant K is [5].

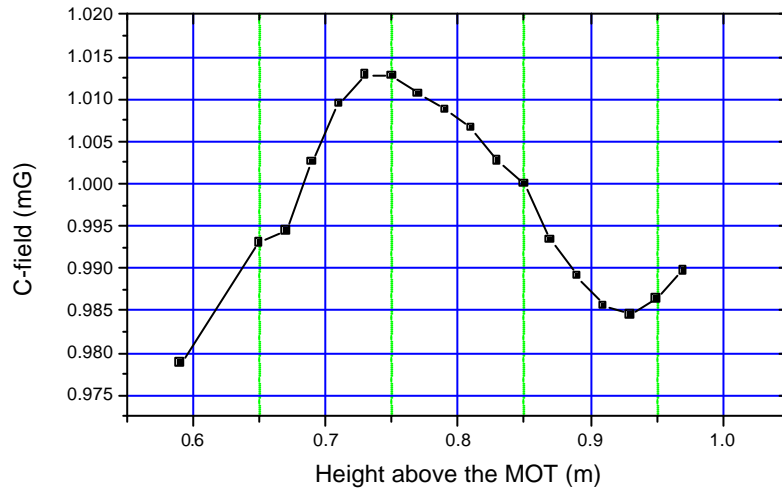


Figure 1. C-field map.

The uncertainty associated to the magnetic field was derived by three independent methods. First, we evaluated the frequency instability of the clock locked on the central fringe of the magnetic sensitive transition $F=3, m_F=-1 \rightarrow F=4, m_F=-1$. This yields to a value that is better than $5 \cdot 10^{-12}$ over on one day of measurement. The instability on the clock transition is $< 1 \cdot 10^{-17}$. Second, the instability of the c-field map was evaluated, mapping before and after the evaluation. This yields to a value of $5 \cdot 10^{-17}$. Third, the uncertainty associated with the map prediction was evaluated. The C field map is used to locate the central fringe of the $F=3, m_F=-1 \rightarrow F=4, m_F=-1$ line. The numerical result agrees with that

obtained following its position at increasing heights better than 0.3 Hz, yielding to a value for the uncertainty on the clock transition frequency of $4 \cdot 10^{-17}$.

The heater used to frequency tune the Ramsey cavity and to stabilize the drift tube temperature is powered with an audio-frequency generator (100 kHz) to avoid the penetration of the generated magnetic field inside the drift tube.

The heater is operated cw during the whole operation cycle of the fountain, in order to prevent a dynamic end-to-end phase shift [6] caused by a temperature modulation of the cavity synchronous with the Ramsey cycle.

Although shielded by several skin depths, a residual rms magnetic field produced by the audio frequency generator could penetrate inside the drift tube, causing a quadratic Zeeman shift of the clock transition frequency.

A calibration of this effect is performed feeding the part of the heater around the drift tube with a calibrated dc current, while the cavities are kept on resonance by the part of the heater around the cavities only (cw at 100 kHz as usual), where the thickness of the copper is larger and the shielding effect is estimated higher by several orders of magnitude.

We measured the magnetic field generated by the heater coils observing the frequency shift of the $F=3, m_F=-1 \rightarrow F=4, m_F=-1$ transition, then we use this value to evaluate the residual magnetic field in the ac condition. The calibration shows that the ac Zeeman shift is less than $4 \cdot 10^{-17}$.

The total uncertainty on the Zeeman shift correction (dc and ac together) is then conservatively stated as $1 \cdot 10^{-16}$.

$$\Delta\nu_Z = K \cdot B_0^2$$

$$K = 427.45 \text{ Hz/T}^2$$

B_0 , C-field as calculated with the map

$$\Delta\nu_Z = (46.0 \pm 0.1) \cdot 10^{-15}$$

Collisional Shift

The collisional shift is evaluated using a continuous differential measurement. The fountain is operated alternatively at high (HD) and low (LD) atomic density and the HM frequency measured in the two configurations is compared. As it was reported in [1], the ratio between the atomic density and the total number of detected atoms is assumed to be constant, then we assume that the collisional frequency shift is proportional to the number of detected atoms.

The differential measurement provides a collisional coefficient which is used to correct the spin-exchange shift on a daily basis with the proper density value as obtained by the detected signal.

During the present evaluation, the fountain is operated at LD or HD density using the MOT loading time (70 ms and 300 ms respectively at LD and HD) as a control parameter: the resulting ratio between the number of detected atoms in the two configurations was about 5. The fountain was continuously operated alternating about 9500 s in the LD and about 2000 s in the HD configuration.

The HM frequency was then extrapolated to the zero atomic density condition, via the relation:

$$y_0 = \frac{R}{R-1} y_{LD} - \frac{1}{R-1} y_{HD} \quad (1)$$

where y_0 is the zero density extrapolation, y_{LD} and y_{HD} are the frequency in LD and HD condition, R is the ratio between the number of atoms in HD configuration (N_{HD}) and the number of atoms in LD configuration (N_{LD}).

The y_0 extrapolation is calculated for each couple of LD-HD runs (total duration 11500 s), allowing a high level rejection of the effects (long term fluctuations of HM frequency, MOT loading efficiency and atom detection efficiency) which can introduce biases to the y_0 value calculated with (1).

The type A uncertainty associated to the measurement is then obtained from equation (1):

$$s_{y_0}^2 = \left(\frac{R}{R-1} \right)^2 s_{y_{LD}}^2 + \left(\frac{1}{R-1} \right)^2 s_{y_{HD}}^2 + s_R^2 \left(\frac{y_{LD} - y_{HD}}{(R-1)^2} \right)^2 \quad (2)$$

Another contribution to the collisional shift uncertainty is reported in the Type B budget. This contribution is mainly due to the hypothesis about the linear relation between the atomic density and the detected signal and to a non-complete rejection of long term effects. This assumption is evaluated to be correct at the level of 15% .

During the present evaluation, the average value of the cold collision relative frequency shift and the associated type B uncertainty were:

$$\Delta\nu_{\text{Coll}} = (-1.2 \pm 0.2) \cdot 10^{-15}$$

Other Shifts

The actual influence of other shifts resulting from several physical and technical effects was carefully investigated during the most recent history of IEN-CsF1. The contribution of these shifts is either negligible or not easily modelled and then no correction is applied for. Only an uncertainty contribution is provided for these effects, reflecting the estimation of their maximum values during the fountain operation.

These shifts, either theoretically estimated or measured, are [1]

- Resonant light shift
- Distributed cavity shift
- Dynamic end-to-end phase shift
- Cavity pulling
- Relativistic Doppler shift
- Synthesizer and numerical loop errors
- Microwave leakage and power-related shifts

Before the evaluation here reported, tests were conducted in order to estimate the shift and the uncertainty contributions of the microwave leakage during the operation of IEN-CsF1. All the possible sources of microwave leakage were carefully surveyed. Leverage tests, conducted operating the fountain with a high microwave power level, provide an estimation of the possible leakage shift.

As it was recently reported [7], the relation between the microwave field amplitude and the leakage induced shift is not linear and can be dramatically different if the leakage occurs between the two Ramsey interrogations or after that, before the detection stage.

For these reasons, leverage tests were designed following the theory reported in [7], and different tests were conducted to estimate the shift due to the leakage during different stages of the fountain cycle.

The estimation of the microwave leakage shift is zero with an uncertainty of $0.5 \cdot 10^{-15}$

Summary of accuracy evaluation

| Effect | Shift (10^{-15}) | Uncertainty (10^{-15}) |
|------------------------------------|--------------------------------------|--|
| 2 nd order Zeeman Shift | +46.0 | 0.1 |
| Blackbody Radiation Shift | -29.9 | 0.1 |
| Gravitational Red Shift | +26.4 | 0.1 |
| Microwave Leakage Shift | -- | 0.5 |
| Collisional Shift (Systematic) | -1.2 (*) | 0.2 |
| Other shifts | -- | 0.1 |
| Total | +41.3 | 0.6 |

Table 1. Summary of corrected and uncorrected shifts and uncertainty budget for IEN-CsF1, period MJD 53639-53664. (*) Average value.

Evaluation of the average frequency $y(IEN-CsF1)-y(HM2)$

During the reported evaluation period, at IEN only one H-maser was running (BIPM code 1401102), as the other one (BIPM code 1401101) was unavailable because of maintenance.

The average frequency $y(IEN-CsF1)-y(HM2)$ over the period MJD 53639.0-53664.0 was calculated with a linear fit on the $y(IEN-CsF1)-y(HM2)$ data, coming from each individual fountain run corrected for the collisional shift. As these data have different Type A uncertainties, we used a weighted least square algorithm. The fit method was chosen because fountain dead (lost) time is unavoidable during the evaluation period, and the dead time intervals are neither evenly spaced nor symmetric with respect to the centre of the evaluation period. In these conditions, dead time would have biased an estimation derived by a standard average [8]. Epoch distribution of fountain dead time is reported in Figure 2.

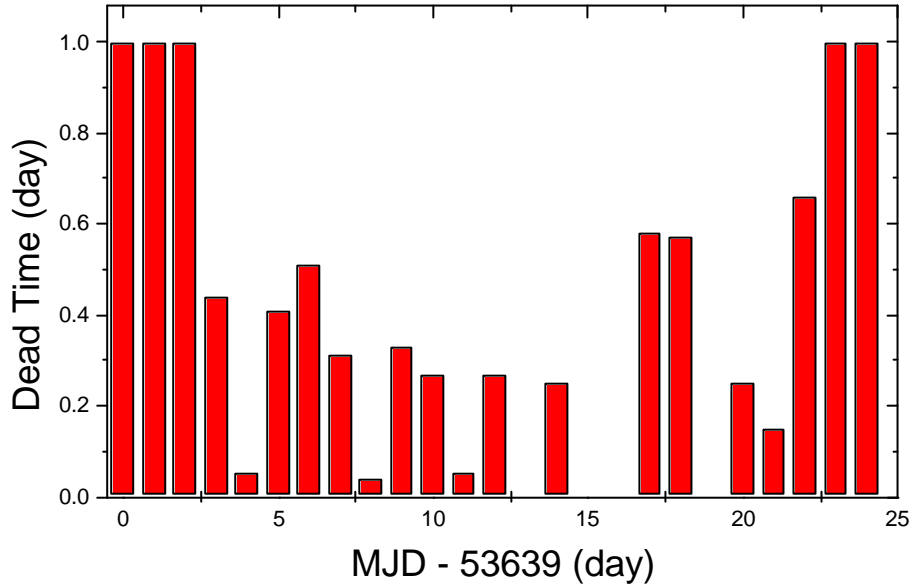


Figure 2. Epoch distribution of the dead time during the present evaluation.

$y(IEN-CsF1)-y(HM2)$ data are fitted with the linear model:

$$Y = At + B \quad (1)$$

The choice of a linear model takes into account the fact that the HM2 frequency has shown a very stable drift in the past two years within periods even larger than 40 days. Moreover, we tried to fit the data with a quadratic model; in this case the second order coefficient estimated by the fit was compatible with zero.

The estimation of the average frequency $y(IEN-CsF1)-y(HM2)$ during the evaluation interval is $Y|_{t=t_0}$ where t_0 is the evaluation period centre (MJD 53651.5 in this particular case). If the epoch coordinate origin is taken on the centre of the evaluation interval, the coefficient B, as it is estimated by the weighted least square algorithm, corresponds to the estimation of the average frequency $y(IEN-CsF1)-y(HM2)$ during the evaluation interval.

The linear fit is weighted on the squared Type A uncertainty of each $y(IEN-CsF1)-y(HM2)$ datum. The uncertainty of each datum includes both the uncertainty due to the fountain stability and the uncertainty due to the collision shift evaluation (Type A contribution). The uncertainty associated to the average frequency estimation $y(IEN-CsF1)-y(HM2)$ and reported as Type A uncertainty is the uncertainty of the coefficient B as it is estimated by the weighted least square algorithm. Figure 3 reports $y(IEN-CsF1)-y(HM2)$ data, corrected for the total shift reported in Table 1, and the linear fit curve.

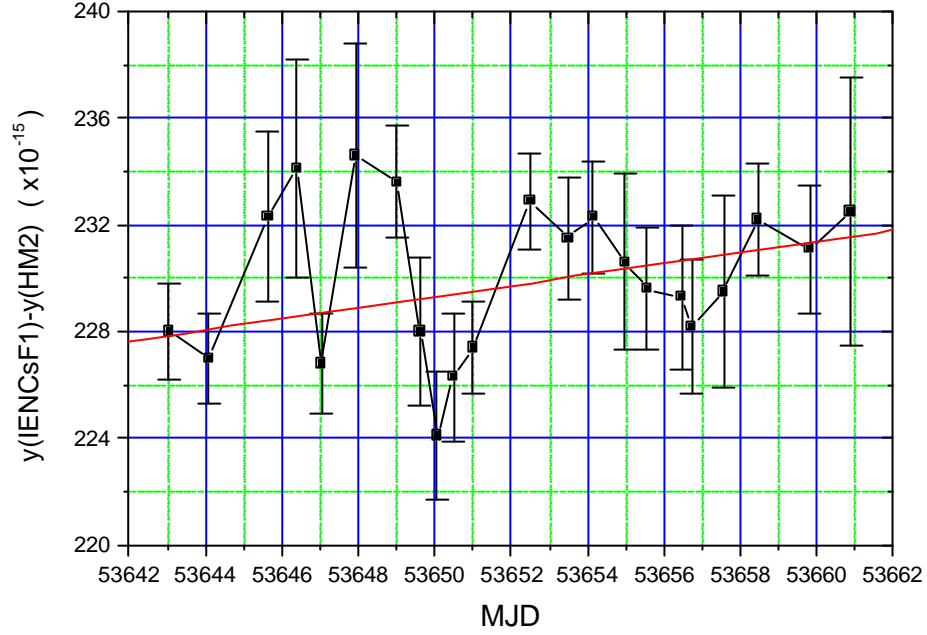


Figure 3. $y(IEN-CsF1)-y(HM2)$ data (squares) and the linear fit curve (straight line).

The linear regression provides the best estimation when the expression (1) is the correct model for the maser drift and the fit residuals are dominated by white frequency noise. As no high stability local oscillator other than HM2 was running at IEN during fountain evaluation period, it is difficult to prove the two positions reported above. However, with the help of all the data collected during the past fountain evaluations and the operative life of HM2 [9], one can reasonably assess that, for a 25 days long period, the fit residuals are dominated by the white frequency noise of the fountain and higher order drifts of the maser are negligible. Final results of the statistical analysis is reported in Table 2:

| | Value | Uncertainty |
|---------------|----------------------------|----------------------------|
| Coefficient A | $0.21 \cdot 10^{-15}$ /day | $0.11 \cdot 10^{-15}$ /day |
| Coefficient B | $+229.6 \cdot 10^{-15}$ | $0.6 \cdot 10^{-15}$ |

Table 2. Results of the weighted linear fit $y=At+B$.

Local link and dead time uncertainty (ul/lab)

The HM2 is phase compared to UTC(IEN) time scale, which is the reference time scale for remote time and frequency transfer tools, with a Time Interval Counter in the IEN Time and Frequency laboratory. This comparison introduces a uncertainty contribution to the IEN-CsF1 transfer to TAI, which is estimated as $<0.1 \cdot 10^{-15}$ for this evaluation period (25 days).

Dead time in fountain operation introduces a further uncertainty to the frequency transfer to TAI. The estimation of this uncertainty contribution requires the knowledge of the HM2 noise properties.

A conservative estimation is possible using, for example, the stability analysis of the $y(\text{IEN-CsF1})-y(\text{HM2})$ data obtained during the fountain comparison experiment in 2004 [9]. This analysis provides that the stability of HM2 could be modelled in terms of Allan variance, as:

$$\mathbf{s}_y^2(\mathbf{t}) = \mathbf{s}_{yWF}^2(\mathbf{t}) + \mathbf{s}_{yFF}^2(\mathbf{t}) + \mathbf{s}_{yRW}^2(\mathbf{t})$$

where $\sigma_{yWF}^2(\tau)$, $\sigma_{yFF}^2(\tau)$ and $\sigma_{yRW}^2(\tau)$ are respectively the contribution due to white, flicker and random walk frequency noise.

A conservative estimation of these contributions is:

$$\begin{aligned} \mathbf{s}_{yWF}(\mathbf{t}) &= 3 \cdot 10^{-13} \mathbf{t}^{-1/2} \\ \mathbf{s}_{yFF}(\mathbf{t}) &< 3 \cdot 10^{-16} \\ \mathbf{s}_{yRW}(\mathbf{t}) &< 2 \cdot 10^{-19} \mathbf{t}^{1/2} \end{aligned} \quad (3)$$

The dead time uncertainty contribution is calculated with the following formulas [8,10]:

$$\begin{aligned} \mathbf{s}_{dWF}(\Delta T) &= \frac{\mathbf{s}_{yWF}(1s)}{\sqrt{\Delta T}} \sqrt{\frac{x}{1-x}} \\ \mathbf{s}_{dFF} &\approx \sqrt{B_2 B_3 - 1} \mathbf{s}_{yFF} \\ \mathbf{s}_{dRW}(\Delta T) &\approx \sqrt{[(1-x)B_2 B_3 - 1]} \mathbf{s}_{yRW}(1s) \sqrt{\Delta T} \end{aligned} \quad (4)$$

where σ_{dWF} , σ_{dFF} and σ_{dRW} are the contribution to the dead time uncertainty due to white, flicker and random walk frequency noise of the local oscillator; \mathbf{DT} is the evaluation period, $\mathbf{s}(1s)$ is the stability of the local oscillator at 1 s, and x is the fractional dead-time.

$B_2 = B_2(r, \mu)$ and $B_3 = B_3(M, r, \mu)$ are the bias functions defined in [11, 12]: they depend on the three variables μ , M , r , associated respectively to the noise type ($\mu = +1$ flicker frequency noise, $\mu = +2$ random walk frequency noise) to the temporal distribution of the dead time (see Figure 2) and to the fractional dead time via the relation $r=(1-x)^{-1}$.

As the dead time is not regularly distributed, for the B_3 calculation we considered the dead time as lumped ($M=1$), which implies a conservative estimation of the uncertainty.

Considering the values of $\sigma_{y_{WF}}(\tau)$, $\sigma_{y_{FF}}(\tau)$ and $\sigma_{y_{RW}}(\tau)$ reported in the equations (3), and that the amount of that time in the present evaluation is 40%, the bias function coefficients are:

$$B_2(1.67, +1) = 2 \quad B_2(1.67, +2) = 2.8 \quad B_3(1, 1.67, +1) = 1 \quad B_3(1, 1.67, +2) = 1.$$

From Equations (4) it follows that $\sigma_{dWF} = 1.7 \cdot 10^{-16}$, $\sigma_{dFF} = 3 \cdot 10^{-16}$ and $\sigma_{dRW} = 2.5 \cdot 10^{-16}$ and the total uncertainty due to the dead time is evaluated to be $\sigma_d = 4 \cdot 10^{-16}$.

| Contribution | Uncertainty (10^{-15}) |
|---------------------------|--|
| HM link to UTC(IEN) | 0.1 |
| Fountain Dead Time (40 %) | 0.4 |
| Total (ul/lab) | 0.4 |

Table 3. Contributions to ul/lab.

Summary of TAI evaluation results

| MJD Period | y(IENCsF1-HM2) | uA | uB | ul/lab |
|-------------------|------------------------------|----------------------------|-----------------------|-----------------------------|
| 53639-53664 | +229.6·10 ⁻¹⁵ (*) | 0.6·10 ⁻¹⁵ (**) | 0.6·10 ⁻¹⁵ | 0.4·10 ⁻¹⁵ (***) |

Table 4. Final results of IEN-CsF1 evaluation.

(*) HM2 has the BIPM code 1401102

(**) Including collisional shift evaluation uncertainty (Type A contribution)

(***) Including contribution of uncertainties due to the local link to UTC(IEN) and to the fountain dead time.

References

- [1] F. Levi, L. Lorini, D. Calonico, A. Godone, "IEN-CsF1 accuracy evaluation and Two-Way frequency comparison". IEEE Transactions on Ultrasonics, Ferroelectrics, and Frequency Control, vol. 51, no. 10, pp. 1216-1224 (October 2004)
- [2] F. Levi, D. Calonico, L. Lorini, S. Micalizio, A. Godone: "Measurement of the blackbody radiation shift of the ^{133}Cs hyperfine transition in an atomic fountain". Phys. Rev. A, Vol. 70, p. 033412, 2004.
- [3] E. Simon, P. Laurent and A. Clairon, "Measurement of the Stark shift of the Cs hyperfine splitting in an atomic fountain" Phys. Rev. A **57**, 436 (1998).
- [4] S. Micalizio, A. Godone, D. Calonico, F. Levi, L. Lorini: "Blackbody radiation shift of the ^{133}Cs hyperfine transition frequency". Phys. Rev. A, Vol. 69, p. 053401, 2004.
- [5] J. Vanier and C. Audoin, "The Quantum Physics of Atomic Frequency Standards". Bristol/Philadelphia: Adam Hilger, 1989.
- [6] S. R. Jefferts, T. P. Heavner, E. A. Donley and T. E. Parker. "Measurement of Dynamic End-to-End Cavity Phase Shifts in Cesium-Fountain Frequency Standards" IEEE transactions on ultrasonics, ferroelectrics, and frequency control, vol. 51, no. 6, June 2004
- [7] S.R. Jefferts, J.H. Shirley, N.Ashby, E.A. Burt, G.J. Dick, "Power dependence of distributed cavity phase induced frequency biases in atomic fountain frequency standards" To be published in Proc. of 2005 EFTF;
F. Levi, J. Shirley, S.R. Jefferts, "Microwave Leakage Induced Frequency Shifts in the Primary Frequency Standards NIST-F1 and IEN-CSF1". To be published.
- [8] T.E. Parker, D.A. Howe and M. Weiss, "Accurate Frequency Comparisons at the 1×10^{-15} Level," in Proc. 1998 IEEE International Freq. Control Symp., pp 265-272, 1998.
- [9] A. Bauch, J. Achkar, R. Dach, R. Hlavac, L. Lorini, T. Parker, G. Petit, and P. Urich, "Time and Frequency Comparisons Between Four European Timing Institutes And NIST Using Multiple Techniques". To be published in Proc. of 2005 EFTF;
D. Calonico, L. Lorini, F. Levi, "Comparison between remote Cs fountain primary frequency standards". To be published in Proc. of 2005 EFTF
- [10] F. Levi, L. Lorini, D. Calonico, and A. Godone "Systematic Shift Uncertainty Evaluation of IEN-CSF1 Primary Frequency Standard" IEEE Transactions On Instrumentation And Measurement, Vol. 52, No. 2, April 2003
- [11] J. A. Barnes, D. W. Allan, "Variances based on data with dead time between the measurements" NIST Technical Note 1318, 1990
- [12] J.A. Barnes, "Tables of Bias Functions, B_1 and B_2 , for Variances Based On Finite Samples of Processes with Power Law Spectral Densities" NBS Technical Note 375, 1968